

## Many-body effects in a layered electron gas

Pawel Hawrylak,\* Gunnar Eliasson,<sup>†</sup> and John J. Quinn

*Department of Physics, Brown University, Providence, Rhode Island 02912*

(Received 8 July 1987)

Many-body effects in a layered electron gas are studied using the dynamical random-phase approximation. The electron self-energy, effective mass, and lifetime are calculated as functions of electron density and interlayer separation. The results show behavior qualitatively different from that of the interacting electron gas in two and three dimensions.

### I. INTRODUCTION

The relative importance of many-body effects in an interacting electron gas varies as a function of the electron density. For high densities, electron-electron interactions are weak in comparison to the kinetic energy, and they can be treated by perturbative methods like diagrammatic perturbation theory.<sup>1</sup> The small parameter of the perturbation expansion is usually called  $r_s$ . It is the radius (measured in units of the effective Bohr radius) of a sphere enclosing a volume equal to the volume per electron. The perturbative approach can be rigorously justified only for  $r_s \leq 1$ . Unfortunately, most real metals have values of  $r_s$  in the range  $1 \leq r_s \leq 10$  for which no mathematically rigorous methods of treating many-body effects exist. One must rely on different intuitive approximations and hope that they contain the important physics of the properties being investigated. It is difficult to test the validity of these intuitive methods by comparison with experiment because one must go from one metal to another in order to change the electron density. Other effects associated with crystal structure, energy bands, and phonon spectra mask the change associated with the variation in electron density.

The development of metal-insulator-semiconductor (MIS) devices led to an improvement in this situation. In these systems a quasi-two-dimensional electron layer is formed at the semiconductor-insulator interface by the application of a voltage across the insulating layer. The electron density (and  $r_s$ ) can be varied over a wide range of values within a single sample, and the effect of many-body interactions on single-particle properties can be studied experimentally as a function of electron density. The basic structure of the theory of electron-electron interactions in a homogeneous, isotropic electron gas is quite similar in two- and three-dimensional systems. Much experimental and theoretical effort went into studying the excitation spectrum of a two-dimensional (2D) electron gas and its one-electron properties (such as effective mass and  $g$  factor).<sup>2</sup> These experiments proved to be a fruitful test of the validity of various theoretical schemes. It was demonstrated, for example, that when the self-energy is calculated to the lowest order in screened electron-electron interaction, on-shell perturbation theory should be used to estimate the effective mass, and that the local-energy-functional method gave reason-

able results over a wide density range.

Another testing ground for many-body theory is provided by doped semiconductors. By varying the amount of doping the value of  $r_s$  can be varied substantially. Because the effective Bohr radius in semiconductors is large ( $a_0 \sim 10\text{--}100 \text{ \AA}$ ),  $r_s \leq 1$  can easily be achieved. Unfortunately, as demonstrated by Altshuler and Aronov,<sup>3</sup> the effects due to impurities cannot be separated from electron-electron interaction effects. Impurity effects can be greatly reduced in modulation-doping semiconductor superlattices. An excellent example is provided by the GaAs-Ga<sub>x</sub>Al<sub>1-x</sub>As superlattice, where Ga<sub>x</sub>Al<sub>1-x</sub>As layers are doped with Si. Because the bottom of the conduction band of Ga<sub>x</sub>Al<sub>1-x</sub>As is significantly above that of the GaAs layer, electrons "spill" into GaAs layers leaving ionized donors in the centers of the Ga<sub>x</sub>Al<sub>1-x</sub>As layers. In this way layers of quasi-two-dimensional electron gas (LEG) are formed which are spatially separated from the ionized impurities. This results in electronic mobilities several orders of magnitude higher than in bulk semiconductors. These systems offer the hope of reducing the importance of impurity effects and separating them from electron-electron interaction effects. However, because the system is obviously both inhomogeneous and anisotropic, one expects many-body effects to differ from those in a homogeneous, isotropic electron gas in two or three dimensions. As a first step in understanding many-body effects in modulation doped superlattices and other layered compounds, we shall approximate the system by an array of strictly two-dimensional electron gas layers. The layered-electron-gas model (LEG) has been used successfully to study collective excitations (plasmons). Its validity has been confirmed by theoretical calculations<sup>4</sup> and light scattering experiments,<sup>5</sup> and it is interesting to study in its own right. It is well known that plasmons associated with individual layers couple via the long-range Coulomb interaction and lead to the formation of a plasmon band. This structure of collective excitations is peculiar to the LEG and absent in 2D and 3D electron gases. It results both from the anisotropy and periodicity along the superlattice axis. These features make the LEG probably the simplest system qualitatively different from isotropic, homogeneous, jellium models studied so far. It is therefore interesting to see the effects of the plasmon band structure on one-electron properties such as self-energy, effective mass, and inelastic lifetime. These quan-

tities are studied using uncritically the dynamical random phase approximation (RPA). We believe that RPA should give us qualitatively correct features. The more realistic treatment of a superlattice band structure is beyond the scope of this paper as it necessarily involves the question of disorder introduced by impurities in the barriers. The preliminary results of this work have been reported in Ref. 6. This paper is organized as follows: In Sec. II we introduce basic formalism and derive the form of the effective screened interaction: Sec. III describes calculations of the self-energy; the effective mass is dis-

cussed in Sec. IV, and the inelastic lifetime in Sec. V. A discussion and summary of the results are contained in Sec. VI.

## II. THE HAMILTONIAN AND THE EFFECTIVE INTERACTION

The layered electron gas consists of layers of two-dimensional electron gas with 2D density  $n$ , area  $A$ , and separation  $a$ . The Hamiltonian for the LEG has been derived in Ref. 4:

$$H = \sum_{l,k} \epsilon_{k,l} A_{k,l}^\dagger A_{k,l} + \frac{1}{2A} \sum_{k,k',l,l'} \sum_q V^0(l,l') A_{k+q,l}^\dagger A_{k'-q,l'}^\dagger A_{k',l'} A_{k,l}, \quad (1)$$

where  $A_{k,l}$  ( $A_{k,l}^\dagger$ ) is the annihilation (creation) operator for an electron on layer  $l$  in a state characterized by a wave vector in the plane  $k$ .  $V^0(l,l')$  is the two-dimensional Fourier transform of a Coulomb interaction among electrons on layers  $l$  and  $l'$ . That is  $V^0(l,l') = v_q \exp(-q|l-l'|a)$  with  $v_q = 2\pi e^2/\epsilon_0 q$  and  $\epsilon_0$  the background semiconductor dielectric constant. (Note that for brevity we have omitted the dependence of  $V_0$  on  $q$ .) The one-electron properties of the LEG can be derived from a knowledge of the quasiparticle Green's function or the self-energy [Fig. 1(a)]. The case of a three-dimensional electron gas has been treated in detail by numerous authors and our notation and formalism follows very closely that of Mahan.<sup>1</sup> The Matsubara Green's function is defined in the usual way as

$$G(l,l',\tau,p) = -T_\tau \langle A_{p,l}(\tau) A_{p,l'}^\dagger(0) \rangle \delta_{l,l'}, \quad (2)$$

where  $\tau$  is the imaginary time,  $T_\tau$  is the  $\tau$  ordering operator and  $\langle \rangle$  is the thermodynamic average. We note that the exact Green's function is diagonal in layer indices which we have written explicitly. This is because electrons do not tunnel between different layers. It is now easy to rederive the Dyson equation for the Green's function and express it via the bare Green's function  $G^0$  (in the absence of electron-electron interactions) and self-energy  $\Sigma$  as  $G = G^0 + G^0 \Sigma G$ . Retaining only diagrams shown in Fig. 1, the self-energy in RPA can be written as

$$\Sigma_{l,l}(\mathbf{k}, i\omega_n) = -\frac{1}{\beta} \frac{1}{A} \sum_q \sum_{i\omega_n} V(l,l';q, i\omega_n) \times G^0(\mathbf{k}-\mathbf{q}; i\omega_n - i\omega_n), \quad (3)$$

where  $\omega_n = (2n+1)\pi/\beta$  ( $\beta = 1/kT$ ;  $T$  is the temperature) is the fermion frequency.  $V(l,l';q, i\omega)$  is the screened, effective interaction between electrons on layer  $l$ . The two-dimensional Fourier transform  $V(l,l',q, i\omega)$  of the effective interaction for electrons on layers  $l$  and  $l'$  is obtained from the solution of the Dyson equation [diagrammatic representation is shown in Fig. 1(b)]:

$$V(l,l') = V^0(l,l') + \Pi^0 \sum_{l''} V^0(l,l'') V(l'',l'). \quad (4)$$

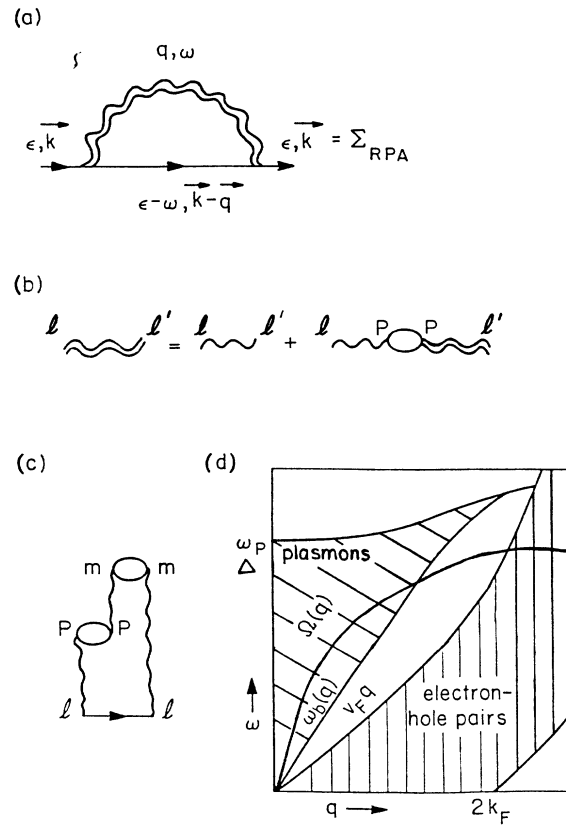


FIG. 1. Schematic representation of relevant diagrams. The straight line corresponds to bare electron Green's function, wiggly line to Coulomb interaction, double wiggly line to screened interaction and indices  $l, l', m$  refer to different layers. (a) gives the RPA self-energy and (b) the Dyson equation for the screened interaction. (c) describes propagation of an electron on layer  $l$  with virtual excitation of electron-hole pairs on layers  $p$  and  $m$  via Coulomb interaction. These processes contribute to the self-energy. (d) schematically maps out the regions of the frequency-wave-vector space corresponding to the finite imaginary part of the screened interaction due to excitation of electron-hole pairs and plasmons. Here  $\Omega(q)$  is the maximum possible energy absorbed by the electron gas for momentum transfer  $q$ .  $\omega_b(q)$  is the bottom of the plasmon band and  $v_F$  is the Fermi velocity. Note that the gap between plasmon and  $e$ - $h$  spectrum can be made arbitrarily small.

Here  $\Pi^0(q, i\omega)$  is the frequency-dependent polarizability of a 2D electron gas

$$\Pi^0(q, i\omega) = \frac{2}{A} \sum_{\mathbf{k}} \frac{f(\epsilon_{\mathbf{k}+\mathbf{q}}) - f(\epsilon_{\mathbf{k}})}{\epsilon_{\mathbf{k}+\mathbf{q}} - \epsilon_{\mathbf{k}} - i\omega}, \quad (5)$$

and  $f$  is the Fermi distribution,  $\epsilon_{\mathbf{k}} = k^2/2m$ ,  $\mathbf{q}$  is the in-plane wave vector,  $m$  is the bare mass and we set  $\hbar=1$ . For an infinite system the interaction depends only on the difference  $l-l'=r$ , i.e.,  $V(l, l') = V(l-l') = V(r)$ . Defining the Fourier transform with respect to the difference in layer indices as  $\phi(k) = \sum_r V(r) e^{ikr}$ ,

$$V(r) = \frac{a}{2\pi} \int_{-\pi/a}^{\pi/a} dk \phi(k) e^{ikra}$$

permits us to reduce Eq. (4) to an algebraic equation for  $\phi(k)$ ,

$$\phi(k) = \phi(k) + \Pi^0 \phi(k) \phi(k). \quad (6)$$

The screened interaction for electrons on a given layer ( $r=0$ ) is now given by

$$V(q, i\omega) = \frac{a}{2\pi} \int_{-\pi/a}^{\pi/a} dk \frac{\phi^0(k)}{1 - \Pi^0(q, i\omega) \phi^0(k)}. \quad (7)$$

For the complex frequency  $i\omega$  the explicit form of the effective interaction is

$$V(q, i\omega) = \frac{v_q \sinh(qa) \operatorname{sgn}[\operatorname{Re}b]}{(b^2 - 1)^{1/2}},$$

$$b = \cosh(qa) - v_q \Pi^0(q, i\omega) \sinh(qa), \quad (8)$$

$$\Pi^0(q, i\omega) = \frac{-2k_F m}{\pi q} \times \left\{ \frac{\epsilon_q}{k_F q / m} - \operatorname{Re} \left[ \left[ \frac{\epsilon_q + i\omega}{k_F q / m} \right]^2 - 1 \right]^{1/2} \right\}.$$

Equation (8) contains information about static and retarded screened interaction. The static screened potential  $V(q, 0)$  is given explicitly by Eq. (8). From Eq. (8) the Thomas-Fermi wave vector for the LEG is  $q_{\text{TF}}^{\text{LEG}} = [(1 + 2a/a_0)^2 - 1]^{1/2}/a$  ( $a_0 = \epsilon_0/e^2 m$  is the effective Bohr radius). For the layer separation  $a$  much larger than the Bohr radius  $a_0$  we recover a single-layer result  $q_{\text{TF}}^{\text{LEG}} = 2/a_0$ . For the separation  $a \leq a_0$  we have  $q_{\text{TF}}^{\text{LEG}} = 2/(aa_0)^{1/2}$ . The range of the screened interaction,  $\sim q_{\text{TF}}^{-1}$ , becomes smaller as the separation between layers decreases. Note that as in two dimensions the Thomas-Fermi wave vector does not depend on electron density on each layer but depends on interlayer separation and hence on the three-dimensional carrier density.

The retarded interaction  $V(q, \omega)$  can be obtained by the analytical continuation  $i\omega \rightarrow \omega + i0^+$  in Eq. (7).  $V(q, \omega)$  reflects the formation of plasmon bands. The imaginary part of  $V(q, \omega)$  is nonzero when  $\operatorname{Im}\Pi^0(q, \omega) \neq 0$  or when  $b \leq 1$  and  $\operatorname{Im}\Pi^0(q, \omega) = 0$ . The first case corresponds to single-particle excitations while the latter describes excitation of plasmons. If we identify  $b = \cos(ka)$  then we recover the well-known dispersion relation for

plasma in a LEG.<sup>4</sup> The phase space  $(q, \omega)$  where there is a nonvanishing imaginary part of  $V(q, \omega)$  due to collective and electron-hole pair excitation is sketched in Fig. 1(d). These results can be also interpreted directly from Eq. (7). Here  $\phi^0(q, k)$  is the three-dimensional Fourier transform of the Coulomb interaction  $V^0(q, r)$ . The denominator in the integrand in Eq. (7) is the standard expression for the RPA dielectric function  $\epsilon(\omega, q, k) = 1 - \phi^0(k, q) \Pi^0(q, \omega + i0^+)$ . Zeros of the dielectric function determine plasmon modes. Plasmons are characterized by the wave vector parallel to the layer  $q$  and perpendicular to the layer  $k$ . Since electrons on a given layer can transfer only momentum parallel to the layer, the screened interaction is averaged over plasmon wave vector  $k$  in the Brillouin zone (BZ). The zeros of  $\epsilon(\omega, q, k)$  give plasmon contribution to the imaginary part of the screened interaction. Since we have a one-dimensional plasmon band, there are square-root divergencies in the plasmon density of states in the center of the BZ and at the BZ edge [ $b = \cos(ka) = \pm 1$  in Eq. (8), respectively] which are seen in the effective, screened interaction.

### III. SELF-ENERGY

The retarded electron self-energy [see Fig. 1(a)] is obtained by the analytical continuation  $i\omega_n \rightarrow \omega + i0^+$  in Eq. (2) and is customarily written<sup>1</sup> as a sum of the line and residue parts  $\Sigma = \Sigma^{\text{line}} + \Sigma^{\text{res}}$ . When we identify the inverse dielectric function as  $1/\epsilon = V/v_q$ , the line and residue contributions at zero temperature are given by

$$\Sigma^{\text{line}}(k, \epsilon) = \int \frac{d^2q}{(2\pi)^2} v_q \int_{-\infty}^{+\infty} \frac{d\omega}{2\pi} \frac{G^0(\mathbf{k}-\mathbf{q}, \epsilon - i\omega)}{\epsilon(q, i\omega)},$$

$$\Sigma^{\text{res}}(k, \epsilon) = \int \frac{d^2q}{(2\pi)^2} v_q \frac{[\Theta(\xi_{\mathbf{k}-\mathbf{q}} - \epsilon) - \Theta(\xi_{\mathbf{k}-\mathbf{q}})]}{\epsilon(q, \epsilon - \xi_{\mathbf{k}-\mathbf{q}})}, \quad (9)$$

$$G^0(k, i\omega) = (i\omega - \xi_{\mathbf{k}})^{-1}.$$

Here  $G^0$  is the unperturbed quasiparticle Green's function and  $\xi_{\mathbf{k}}$  is the bare quasiparticle energy measured with respect to the Fermi level. Note that if we split the self-energy into exchange and correlation parts only the latter depends on the presence of other layers. Instead of calculating the self-energy we shall calculate the difference between the self-energy in the LEG and in a single 2D layer. This is dictated by the fact that the layering effects are important in wave-vector range where RPA is a good approximation and that the phonon contribution should depend weakly on the presence of other layers. We now define the difference between the inverse dielectric functions of a 2D layer embedded in the LEG and in a semiconductor by  $\Delta(1/\epsilon) = 1/\epsilon_{\text{LEG}} - 1/\epsilon_{\text{2D}}$  with  $\epsilon_{\text{2D}} = 1 - v_q \Pi(q, \omega)$ . This difference reflects the polarization of the 3D medium. Using new dimensionless variables,  $x = q/2k_F$  and  $y = m\omega/k_F q$ , the difference between electron self-energy in the LEG and in a single 2D layer  $\Delta\Sigma$  evaluated on the Fermi surface ( $k = k_F, \epsilon = 0$ ) is

$$\Delta\Sigma = \frac{4\sqrt{2}}{\pi} \mathcal{R} \frac{1}{r_s} \int_0^\infty dx \int_0^\infty dy \Delta \frac{1}{\epsilon(x, iy)} \operatorname{Re} \frac{1}{[(iy - x)^2 - 1]^{1/2}}. \quad (10)$$

There  $r_s = (a_0 \sqrt{n\pi})^{-1}$  is the dimensionless, average distance between electrons on the layer and  $\mathcal{R} = e^2/2\epsilon_0 a_0$  is the effective Rydberg constant. Equation (10) is evaluated numerically. In Fig. 2 we show  $\Delta\Sigma$  for a given  $r_s/a_0=1$  as a function of inverse interlayer separation  $a$  (measured in units of  $a_0$ ). The difference in self-energies goes to zero for  $a \geq a_0$  (layers far apart) and increases quite rapidly for  $a \leq a_0$ .  $\Delta\Sigma$  is negative because screening in the LEG is stronger than in a single layer, hence interaction effects are weaker. The  $\Delta\Sigma$  reflects the change in the optical transitions threshold (chemical potential) between valence- and conduction-band states in a superlattice as a function of the superlattice period.

#### IV. EFFECTIVE MASS

We now turn to the effective mass on the Fermi surface. This is a classical problem and for extensive discussion we refer the reader to Ref. 1. Here we use standard perturbation theory which evaluates the self-energy at the bare electron frequency which gives  $m/m^* = 1 + (\partial\Sigma/\partial\epsilon_k + \partial\Sigma/\partial\epsilon)$ , and derivatives are evaluated on the Fermi surface. Starting from Eq. (9), the difference  $\Delta(m/m^*)$  between the LEG and a single layer can now be written as

$$\Delta \left( \frac{m}{m^*} \right) = \frac{\sqrt{2}}{\pi} r_s \int_0^\infty dx \int_0^\infty dy \Delta \frac{1}{\epsilon(x, iy)} \operatorname{Re} \left[ \frac{1}{[(iy-x)^2 - 1]^{3/2}} \right] + \frac{r_s}{\pi\sqrt{2}} \int_0^1 dx \Delta \frac{1}{\epsilon(x, 0)} \frac{1}{x(1-x^2)^{1/2}}. \quad (11)$$

Equation (11) is evaluated numerically. Figure 3 shows  $\Delta(m/m^*)$  as a function of  $r_s$  for  $a/a_0=1$ . For  $r_s=0$  both effective masses are equal to bare masses so  $\Delta(m/m^*)$  starts at zero, decreases as  $r_s$  increases to reach a local minimum and then increases monotonically and becomes positive.  $\Delta(m/m^*)$  shows also an interesting behavior as a function of interlayer separation, for fixed  $r_s$ , as shown in Fig. 4. For  $a \geq a_0$ ,  $\Delta(m/m^*) \rightarrow 0$  but shows a local minimum at some interlayer separation. These predictions can be verified experimentally by measurements of the amplitude of low-temperature Shubnikov-de Haas oscillations in the conductivity<sup>3</sup> or low-temperature electronic specific heat.

#### V. INELASTIC LIFETIME

We now turn to the electron lifetime  $\tau_k$  which is given by  $\tau_k^{-1} = -2 \operatorname{Im}\Sigma(k, \xi_k)$ . The finite lifetime is due to excitation of electron-hole pairs and plasmons. For the quasiparticle close to the Fermi surface,  $k \sim k_F$ , only electron-hole pairs contribute to the lifetime with  $\tau_k^{-1} \sim (k - k_F)^2$  in three dimensions and  $\tau_k^{-1} \sim (k - k_F)^2 \ln(k - k_F)$  in two dimensions.<sup>1,2,7</sup> Plasmons can contribute for excitation energies  $\xi_k$  larger than the critical value  $\Delta_c$ , which is usually a large fraction of the Fer-

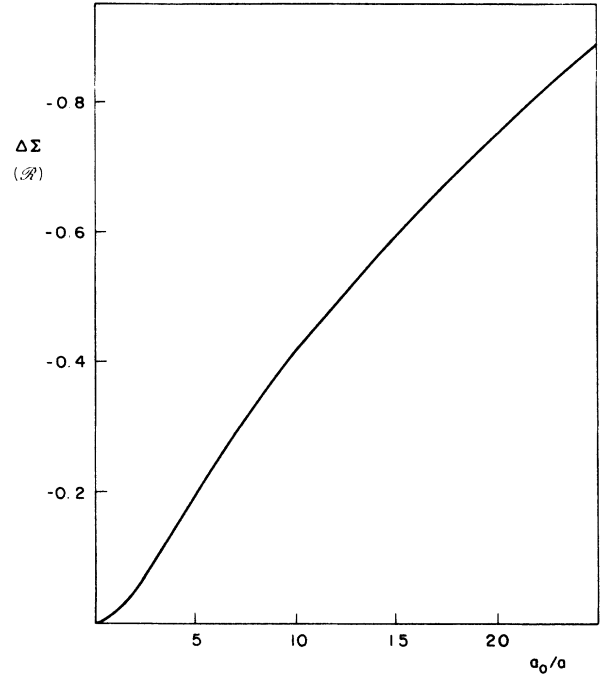


FIG. 2. The difference in self-energy  $\Delta\Sigma$  in the LEG and 2D electron gas as a function of the inverse of the layer separation  $a$  for  $r_s = a_0$ .  $\Delta\Sigma$  is measured in effective Rydberg constant  $\mathcal{R}$  and  $a$  in effective Bohr radius  $a_0$ . Note that  $a^{-1}$  for constant  $r_s$  is proportional to 3D electron density.

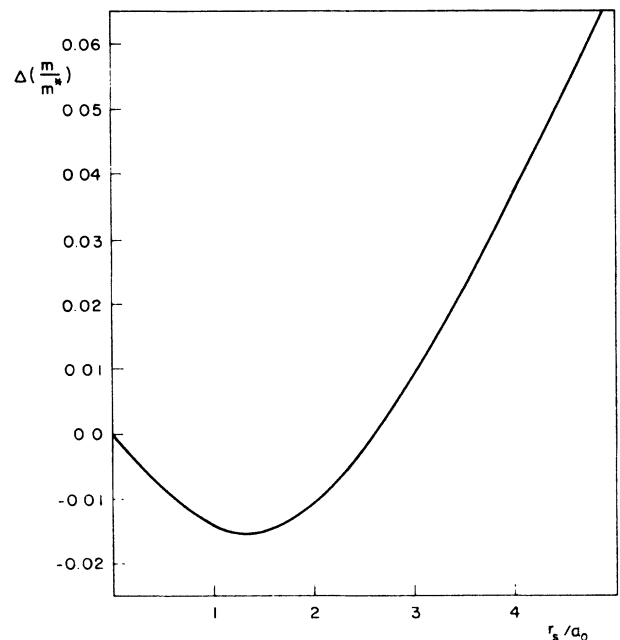


FIG. 3. The difference in inverse effective masses  $\Delta(m/m^*)$  in the LEG and 2D electron gas as a function of  $r_s$  for constant layer separation  $a = a_0$ .

mi energy.

In a 3D electron gas, the plasmon spectrum has a gap, so the quasiparticle excitation energy must be larger than the plasmon energy. In 2 electron gas there is no gap in the plasmon spectrum but the kinematic constraints lead to the excitation threshold. In the LEG there is a possi-

bility of acoustical plasmon emission which, as we shall demonstrate, can occur for arbitrary small excitation energies.

The only contribution to the imaginary part of the self-energy comes from the residue part of the self-energy. From Eq. (9) the quasiparticle lifetime is given:

$$\frac{1}{\tau_k} = 4 \int_0^{2k} \frac{dq q v_q}{(2\pi)^2} \int_0^{\Omega(q)} d\omega \frac{\Theta(\xi_k - \omega)}{\{[\omega - \Omega(q)][\Omega(q) - \omega - 2kq/m]\}^{1/2}} \left[ -\text{Im} \frac{1}{\epsilon(q, \omega)} \right], \quad (12)$$

where  $\Theta(x) = 1$  for  $x \geq 0$ , and zero otherwise;  $\Omega(q) = kq/m - \epsilon_q$ . The imaginary part of  $\tau_k^{-1}$  is nonzero when the imaginary part of the inverse dielectric function is nonzero. We find it convenient to write Eq. (12) in the variables  $x$  and  $y$ . For the plasmon contribution in the LEG we can write

$$1/\tau_k = \mathcal{R} \frac{8\sqrt{2}}{\pi r_s} \int_0^{(k/k_F - 1)/2} dx \int_{y_b(x)}^{\min[y_\Omega(x), y_u(x)]} dy \frac{\sinh(x2\sqrt{2}a/r_s)}{[(y - y_\Omega)(y_\Omega - y - 2k)]^{1/2}} \frac{1}{(1 - b^2)^{1/2}}. \quad (13)$$

Here  $y_b(x)$  and  $y_u(x)$  correspond to lower and upper plasmon band edges:  $b(x, y_b) = -1$  and  $b(x, y_u) = +1$ , while  $y_\Omega = k/k_F - x$ . There are three square root divergencies associated with the integrand, at  $b = \pm 1$  and at  $y = y_\Omega$ . The first two are due to the plasmon band and the third is due to the integration over the angle in Eq. (9). The plasmon bands in the  $x$ - $y$  plane are shown in Fig. 5 for  $a/a_0 = 2$ ,  $a/a_0 = 8$ , the single layer, and the classical approximation  $\omega = [(2\pi e^2/\epsilon m)q]^{1/2}$ . The line  $y = 1 + x$  determines the onset of the electron-hole continuum. Let us for definiteness consider the case  $a/a_0 = 2$ .

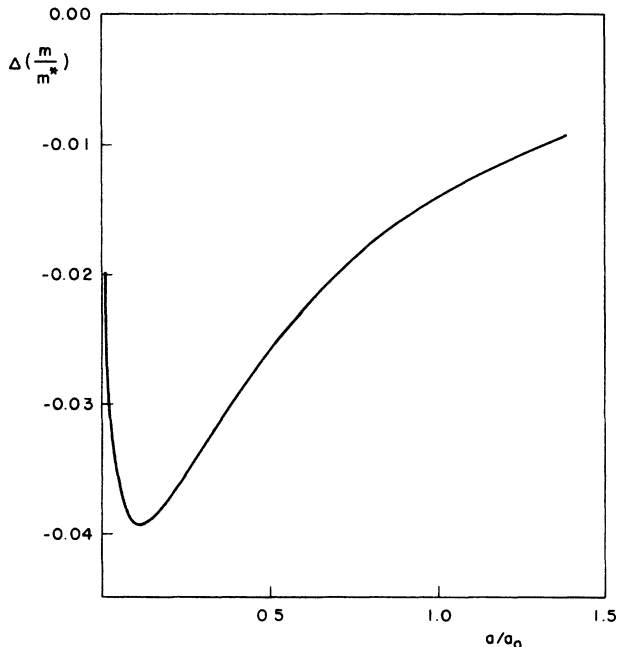


FIG. 4.  $\Delta(m/m^*)$  as a function of layer separation for constant  $r_s/a_0 = 1$ .

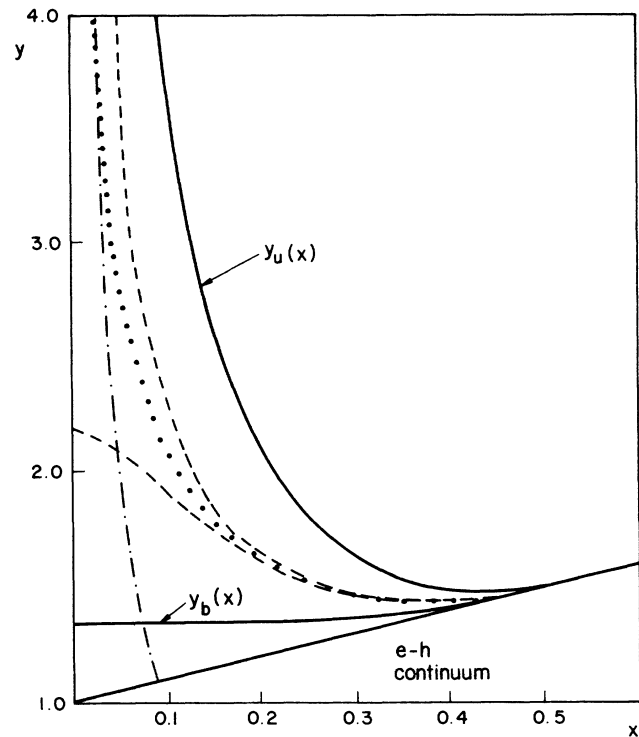


FIG. 5. Plasmon dispersion  $y$  vs  $x$  ( $y = m\omega/qk_F$ ,  $x = q/2k_F$ ) for the layered electron gas with  $r_s = a_0$  and  $a = 2a_0$  (solid lines) and  $a = 8a_0$  (dashed lines). The upper lines  $y_u(x)$  correspond to plasma oscillations in phase ( $k = 0$ ) on different layers while the lower lines  $y_b(x)$  correspond to out of phase ( $k = \pi/a$ ) plasma oscillations on subsequent layers. Plasmon with different wave vectors  $k$  ( $0 \leq k \leq \pi/a$ ) fill the space between  $y_b$  and  $y_u$  lines. Note that acoustical plasmons correspond to the dispersion  $y(x) = \text{const}$ . For comparison this figure includes a 2D plasmon dispersion  $y_p(x)$  in RPA (dotted line) and in classical approximation (dot-dashed line). Note that the plotting  $y$  vs  $x$  instead of  $\omega$  vs  $q$  emphasizes the high-frequency, large wave-vector behavior (both  $y$  and  $x$  are dimensionless).

This case corresponds to the acoustic plasmon emission. For  $y_\Omega > y_b(0)$  we can approximate

$$(1-b^2)^{1/2} \approx 2 \left[ \frac{\delta b}{\delta y} \Big|_{y=y_b} \right] [y - y_b(0)] ;$$

and  $y_\Omega - y - 2k \approx -2k$ . This allows us to write the acoustic plasmon contribution [acoustic plasmons correspond to the dispersion  $y(x) = \text{const}$ ] as

$$\frac{1}{\tau_k} \approx \mathcal{R} \frac{16}{\pi \left[ \left[ \frac{\delta b}{\delta y} \Big|_{y=y_b(0)} \right]^{1/2} (k_c/k_F)^{1/2} \frac{a}{r_s^2} \right]} \times \int_0^{(k-k_c)/k_F} dx x \int_{y_b}^{y_\Omega(x)} \frac{dy}{[(y_\Omega - y)(y - y_b)]^{1/2}} . \quad (14)$$

The critical value of the wave vector above which acoustic plasmons contribute to the inelastic lifetime is given by  $y_b(0) = k_c/k_F$ . The  $y$  integral is  $x$  independent and equal to  $\pi$ , so Eq. (14) predicts the wave-vector dependence of  $\tau_k^{-1}$  as

$$\tau_k^{-1} \approx \frac{8\mathcal{R}\sqrt{a}}{\sqrt{2}r_s^2} \left[ \frac{1+1/a}{(1+1/a)^2 - 1} \right]^{3/2} \left[ \frac{k-k_c}{k_c} \right]^2 , \quad (15)$$

$$k_c = k_F \frac{1+1/a}{(1+1/a)^2 - 1} .$$

Hence acoustical plasmons contribute to the inverse lifetime as  $\tau_k^{-1} \sim (k-k_c)^2$  and the critical wave vector  $k_c$  can be made very close to  $k_F$  by decreasing interlayer separation. The rapid increase  $\tau_k^{-1}$  due to acoustic plasmon emission terminates at the value of the wave vector  $k^*$ . This value is determined by the condition  $y_\Omega = y_u$  and  $\delta y_u / \delta x = -1$ , i.e., the  $y_\Omega$  line becomes tangential to the upper plasmon band edge. For  $k \geq k^*$ ,  $\tau_k^{-1}$  decreases as a function of  $k$ . This behavior is illustrated in Fig. 6 (solid line) where we show the results of the numerical integration of Eq. (13) for  $a/a_0 = 2$ ,  $r_s/a_0 = 1$ . For these values the acoustic plasmon emission threshold, Eq. (15), gives  $k_c = 1.34k_F$  and the maximum

$$1/\tau_k = \mathcal{R} \frac{8\sqrt{2}}{r_s} \int_{x_1}^{x_2} dx \frac{1}{\frac{\delta \epsilon}{\delta y}(x, y_p(x)) \{ [y_p(x) - y_\Omega(x)] [y_\Omega(x) - y_p(x) - 2k] \}^{1/2}} . \quad (16)$$

Here  $y_p(x)$  is the 2D plasmon dispersion, shown in Fig. 5, for  $r_s = 1$ . The range of  $x$  integration ( $x_1, x_2$ ) is given by the solution  $y_p(x_{1,2}) = y_\Omega(x_{1,2})$ . The two solutions exist for the wave vector larger than a critical value  $k_c$ . For  $r_s = 1$  the value of  $k_c$  is  $1.76k_F$ . For  $k = k_c$ , the  $y_\Omega(x)$  line is tangential to the plasmon curve  $y_p(x)$  at  $x = x^*$ . For  $k \geq k_c$  we can expand the plasmon dispersion in the vicinity of the critical point  $x^*$ :  $y_p(x) \approx y_p(x^*) - (x - x^*) + \frac{1}{2} y_p''(x^*)(x - x^*)^2$ ; where we have made the use of the fact that  $y_p'(x^*) = -1$ . It is easy to see that  $y_\Omega(x) - y_p(x) \approx (x - x_1)(x_2 - x)$  where  $x_{1,2} = x^* \pm [(k$

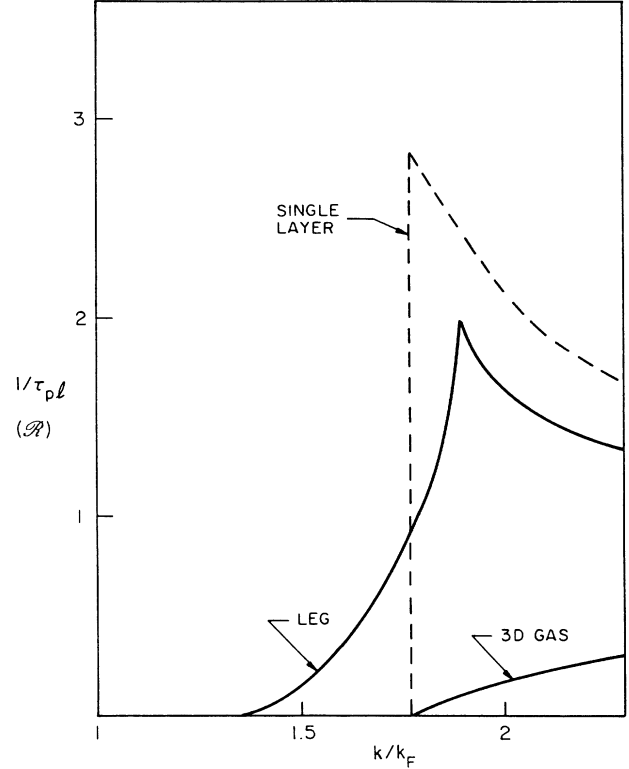


FIG. 6. Inverse lifetime of quasiparticles due to plasmon emission as a function of the wave vector in the LEG with  $a = 2a_0$  and  $r_s = a_0$ , single layer with  $r_s = a_0$  and 3D electron gas with the same bulk density as the LEG. Note that acoustical plasmons contribute to quasiparticle lifetime at lower wave vectors than plasmons in two dimensions and three dimensions. Also note a discontinuous rise in  $\tau_k^{-1}$  for a single layer as opposed to a smooth behavior in three dimensions.

imum value of  $\tau_k^{-1}$  is at the value  $k^* = 1.88k_F$ .

To understand the role of plasmon emission in LEG with large interlayer separation, we must first discuss plasmon emission in strictly 2D systems. In a 2D electron gas the plasmon is given by the zero of the dielectric function  $\epsilon(q, \omega) = 1 - v_q \Pi^0(q, \omega)$  or the pole in the inverse dielectric function. Using Eq. (9) the plasmon contribution to  $\tau_k^{-1}$  in two dimensions can be written as

$-\frac{1}{2} y_p''(x^*)]^{1/2}$  so that the  $x$  integral is  $k$  independent and equal to  $\pi$ . For  $k > k_c$  we therefore find  $\tau_k^{-1}$  to be a constant,

$$\tau_k^{-1} \approx \begin{cases} \mathcal{R} \frac{8\pi\sqrt{2}}{r_s \frac{\delta \epsilon}{\delta y}(x^*, y_p''(x^*)) [\frac{1}{2} y_p(x^*)]^{1/2}} , & k > k_c \\ 0 , & k < k_c . \end{cases} \quad (17)$$

Hence, plasmon contribution to the imaginary part of the

self-energy results in a discontinuous jump at a critical wave vector. The results of numerical integration of Eq. (15) are shown in Fig. 6. The existence of this sharp feature is associated with complex plasmon dispersion for large wave vectors and frequencies.<sup>8</sup> If we use classical approximation for plasmon dispersion  $\omega_p \sim q^{1/2}$ , we have  $\tau_k^{-1} \sim (k - k_c)^{1/2}$ .<sup>7</sup> That is there is no discontinuity in  $\tau_k^{-1}$ . It is worthwhile to mention that in three dimensions there is a threshold for plasmon emission, but  $\tau_k^{-1}$  is a continuous, smooth function of the wave vector.<sup>9</sup> This can be predicted on the basis of classical approximation for plasmon dispersion, and this conclusion survives the scrutiny of a more rigorous treatment.<sup>10</sup> In two dimensions the classical approximation (and for that matter hydrodynamic) of the plasmon dispersion fails to give a qualitatively correct description of quasiparticle properties. The comparison of plasmon contribution to  $\tau_k^{-1}$  in two dimensions, three dimensions, and LEG's with identical bulk density is shown in Fig. 6.

The inverse lifetime includes also contributions from the electron-hole pair excitation. The results of a numerical integration of Eq. (12), including plasmon and electron-hole contribution for the LEG with  $a/a_0=2$ ,  $r_s/a_0=1$ , and a 2D system with  $r_s/a_0=1$  (same as Fig. 6) are shown in Fig. 7. It is clear that plasmon contribution dominates the large wave-vector dependence. The small wave-vector dependence shows logarithmic correction but we have not investigated the dependence of these

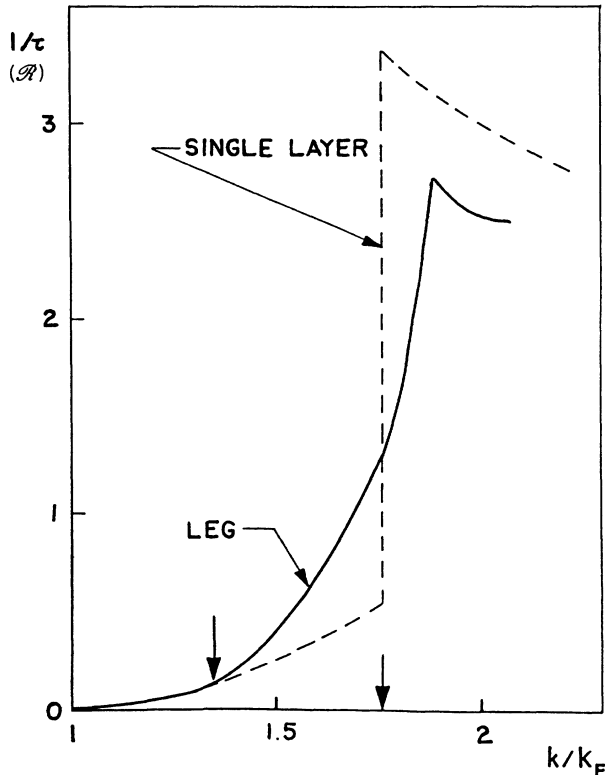


FIG. 7. Inverse lifetime of quasiparticles in LEG and a single layer including plasmon and electron-hole pair contributions. All parameters as in Fig. 6. Arrows indicate the onset of plasmon emission.

corrections on layer separation. The results for  $a/a_0=8$  and  $r_s/a_0=1$  are indistinguishable from the 2D results. This means that as separation between layers increases, acoustic plasmons cease to be an effective decay channel. This happens for a particular value of  $a=a^*$ , which is a function of  $r_s$ .  $a^*$  can be determined from the conditions:  $y_\Omega(0)=y_b(0)$ ,  $y_\Omega(x_0)=y_b(x_0)$ , and  $y_\Omega(x_0)=-1$ . The dependence of  $a^*$  on  $r_s$  is shown in Fig. 8. For  $a < a^*$  acoustic plasmons contribute to the spectrum, while for  $a > a^*$  the spectrum resembles that of a 2D system. It can be shown that for  $a > a^*$ ,  $\tau_k \sim (k - k_c)^{1/2}$  where  $k_c$  is the critical wave vector for high-frequency, lower-band-edge plasmon emissions. This behavior persists for  $k$  up to  $k^*$ .

## VI. SUMMARY AND CONCLUSIONS

We have investigated electron-electron interaction effects in a layered electron gas using dynamical RPA. The layered electron gas is an excellent example of a simple yet highly anisotropic, inhomogeneous, interacting, many-body system. The screened interaction reflects the existence of a plasmon band. The collective excitations do not appear as isolated singularities but as a continuous, though finite, spectrum of the screened interaction. The effective interaction can be varied by changing the electron density or layer separation. The effects of layering on one-electron properties are studied. The dependence of the electron self-energy on a Fermi surface is predicted. The dependence of the effective mass on the Fermi surface on density and layer separation is calculat-

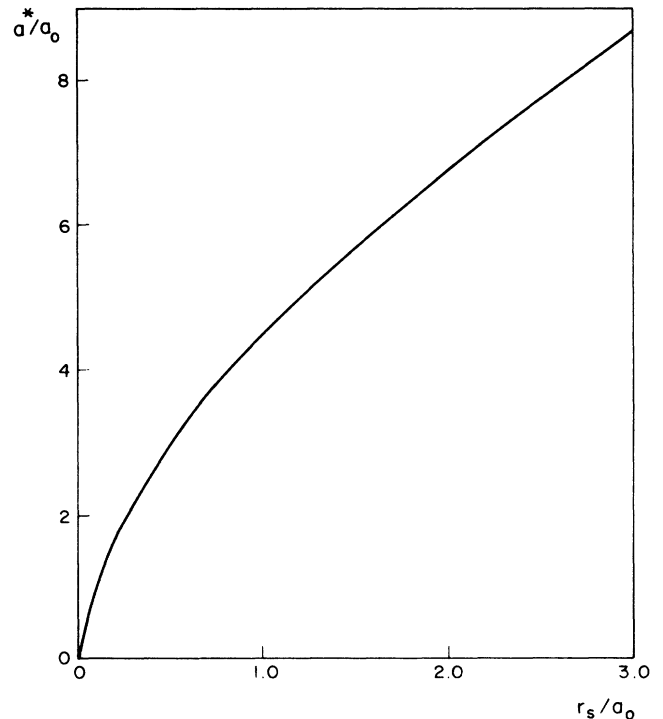


FIG. 8. The dependence of the critical layer separation  $a^*$  on  $r_s$ . For  $a \leq a^*$  acoustical plasmon emission dominates the low-energy spectrum of the inelastic lifetime.

ed. The effective mass can be varied and optimized by changing the interlayer separation. The most interesting effects are found for the imaginary part of the self-energy, or inelastic mean free path and lifetime. It is predicted that in two dimensions the imaginary part of the self-energy as a function of energy changes in a discontinuous way for some energy which is a substantial fraction of the Fermi energy. In LEG, acoustical plasmons become an efficient decay channel. This channel becomes available for very small excitation energies and should therefore affect low-temperature transport properties.

We wish to stress at this point that the LEG model cannot be directly applied to some systems, e.g., semiconductor superlattices with finite barrier heights when interlayer separation becomes very small. In this limit we should approach a bulk, 3D, doped semiconductor. It is

our goal to study the LEG model in order to predict its properties and set the limits on what can be achieved in real materials. This model is sufficiently general to include a broad range of layered materials including semiconductor superlattices, intercalated graphite and high-temperature superconductors.<sup>11</sup> Despite the limitations of the LEG model and the RPA,<sup>12</sup> we expect that the qualitative features discussed here should survive the scrutiny of a more rigorous and complete approach.

#### ACKNOWLEDGMENTS

One of us (P.H.) would like to thank Professor A. Houghton for discussions. This work was supported by the U.S. Army Research Office, Durham, NC, and by the Office of Naval Research.

\*Present address: Division of Physics, NRC, Ottawa, Ontario, Canada K1A 0R6.

†Present address: Laboratory for Atomic and Solid State Physics, Cornell University, Ithaca, NY 14853.

<sup>1</sup>J. J. Quinn and R. A. Ferrell, *Phys. Rev.* **112**, 812 (1958); G. D. Mahan, *Many Particle Physics* (Plenum, New York, 1981).

<sup>2</sup>C. S. Ting, T. K. Lee, and J. J. Quinn, *Phys. Rev. Lett.* **34**, 870 (1975); B. Vinter, *Phys. Rev. B* **15**, 3947 (1977); M. Jonson, *J. Phys. C* **9**, 3055 (1976); A. V. Chaplik, *Zh. Eksp. Teor. Fiz.* **60**, 1845 (1971); T. K. Lee, C. S. Ting, and J. J. Quinn, *Phys. Rev. Lett.* **35**, 1048 (1975); J. L. Smith and P. J. Stiles, *ibid.* **29**, 102 (1972); for a review and full references see T. Ando, A. B. Fowler, and F. Stern, *Rev. Mod. Phys.* **54**, 436 (1982).

<sup>3</sup>B. L. Al'tshuler and A. G. Aronov, *Zh. Eksp. Teor. Fiz.* **77**, 2028 (1979) [*Sov. Phys.—JETP* **50**, 968 (1979)]; for a review see P. A. Lee and T. V. Ramarakrishnan, *Rev. Mod. Phys.* **57**, 287 (1985).

<sup>4</sup>D. Grecu, *Phys. Rev. B* **8**, 1958 (1973); S. Das Sarma and J. J. Quinn, *ibid.* **25**, 7603 (1982); A. C. Tselis and J. J. Quinn, *ibid.* **29**, 3318 (1984); J. K. Jain and P. B. Allen, *Phys. Rev.*

*Let.* **54**, 2437 (1985); G. F. Giuliani and J. J. Quinn, *ibid.* **51**, 919 (1983); P. Hawrylak, J.-W. Wu, and J. J. Quinn, *Phys. Rev. B* **32**, 4272 (1985); G. Eliasson, P. Hawrylak, and J. J. Quinn, *ibid.* **35**, 5569 (1987).

<sup>5</sup>R. Sooryakumar, A. Pinczuk, A. Gossard, and W. Wiegmann, *Phys. Rev. B* **31**, 2578 (1985); A. Pinczuk, M. G. Lamont, and A. C. Gossard, *Phys. Rev. Lett.* **56**, 2092 (1986); G. Fasol, N. Mestres, H. P. Hughes, A. Fischer, and K. Ploog, *ibid.* **56**, 2517 (1986).

<sup>6</sup>P. Hawrylak, *Phys. Rev. Lett.* **59**, 485 (1987).

<sup>7</sup>G. F. Giuliani and J. J. Quinn, *Phys. Rev. B* **26**, 4421 (1982).

<sup>8</sup>Qualitatively similar conclusions are reached when Hubbard approximation is used.

<sup>9</sup>J. J. Quinn, *Phys. Rev.* **126**, 1453 (1962).

<sup>10</sup>B. I. Lundqvist, *Phys. Status Solidi* **32**, 273 (1969).

<sup>11</sup>For a role of plasmons in high  $\tau_c$  superconductivity, see, e.g., V. Kresin, *J. Mater. Res.* **2**, 793 (1987).

<sup>12</sup>For recent work beyond RPA in 3D electron gas, see, e.g., G. Vignale and K. S. Singwi, *Phys. Rev. B* **32**, 2156 (1985), and X. Zhu and A. W. Overhauser, *ibid.* **33**, 925 (1986).